The Use of In-line Quantitative Analysis to Follow Polymer Processing

*Sebastião V. Canevarolo,**[1] *Marcelo K. Bertolino,*[1] *Luís A. Pinheiro,*[2] *Vincenzo Palermo,*[3] *Stefano Piccarolo*[3]

Summary: In this work it is presented three applications of real time analysis during extrusion process using an optical device developed by our research group, which applies the concepts of light extinction. Monitoring of polymer blends morphology takes place to infer data concerned to dispersed phase size and concentration. The detector also enables information about melting temperature of polymer during extrusion and the level of viscous heating, and the exfoliation step during processing of a polymer-clay nanocomposite.

Keywords: extrusion; in-line measurements; nanocomposites; polymer blend morphology; viscous heating

Introduction

The literature shows increasing interest in real time analysis of materials during processing step. Real time analysis includes qualitative and quantitative determination of the blend composition, rheological characteristics, molecular structures and morphological parameters.[1–6] These trends have taken place because the so-called off-line measurements are often time-consuming and expensive. Besides this, the off-line measurements sometimes are not representative because the sample preparation and quantification may need completely different environments, which can cause substantial changes from the original state. In real-time analysis the material is characterized in real time during the processing step. The results might be correlated with operational parameters through models obtained from calibration methodologies.

We have developed in-line optical methods to access the extruder performance via analyzing the residence time distribution (RTD) curve.[7,9] The RTD is commonly determined by the response technique to a pulsed input in which a marker (or tracer) is fed instantly to the melt flow and its concentration measured as a function of the time at the die exit. This technique can be used to monitor the presence and size of a second phase during the preparation of blends and composite including nanocomposites via polymer melt compounding.[9–11] The light extinction level (turbidity) measured by the intensity of the detector's signal is dependent upon the second phase type, concentration and particle size. We have used such an apparatus to follow in-line the formation of compatibilized PP/PA6 blends, the melting of the PA6 component in a PP/PA6 blend and the dispersion/exfoliation of MMT mineral clay into a PP nanocomposite.

Detection System

The detection system described in this paper was developed by Mélo and Cane-

[1] Department of Materials Engineering, Federal University of São Carlos, Rod. Washington Luís, km 235, 13565-905, São Carlos, SP Brazil.
Fax: +55 16 33615404;
E-mail: caneva@power.ufscar.br
[2] Department of Materials Engineering, State University of Ponta Grossa, Ponta Grossa, Paraná, Brazil
[3] Department of Chemical Engineering of the Processes and Materials, Università Degli Studi di Palermo, Palermo, Italy

varolo,[7,8] and was first used to follow in-line the residence time distribution during polymer extrusion. During these studies, it was verified that the detector was also able to infer data concerned to characteristics of polymer blends dispersed phase.[9] Pinheiro et al.[10,11] improved the earlier version and explored this feature of the detector and observed that the detector' signal was influenced by concentration and size of dispersed phase during extrusion of a PP/PA6 blend.

The detector consists of a hollow slit die coupled to the extruder (Figure 1). At the bottom position it is placed an incandescent lamp that emits the light which reaches the material being extruded. At the top position there is a CdS photocell, which absorbs the transmitted light from the interaction with the polymer. The attenuation factor or transmittance (T) is given by the ratio between transmitted and incident light intensity (I and I_0, respectively) of transmitted light. T is also function of concentration and size of dispersed phase, according to the Eq. 1:

$$\frac{I}{I_0} = T = \exp(-N \cdot C_{ext} \cdot t) = \exp\left(-\frac{6 \cdot \phi}{\pi \cdot D^3} . C_{ext} . t\right) \quad (1)$$

where N is the number of particles per volume, C_{ext} is the extinction cross-section, t is the optical path thickness, ϕ the volumetric fraction of particles and D the average particle diameter. Thus, the attenuation factor, and so, the transmitted light intensity decreases in a medium with greater particle concentration or having lower particle size.[12]

This detection system can be used in the transient methodologies, where the mixtures are analyzed through its addition in the extruder as a pulse. These methodologies are suitable because they provide fast response and uses small quantities of dispersed phase. However, it is necessary a previous calibration and the use of constant amounts of pulse.[10,11]

The purpose of this paper is to discuss applications of this detection system, such as the following of reactive processing, nanocomposite intercalatin and expholiation, and heat build-up monitoring during extrusion.

Reactive Processing Monitoring

The morphology is an important feature that enables the understanding of polymer mixtures' properties,[13] such as polymer blends, composites, and most recently nanocomposites. These properties are deeply affected by the size, concentration, shape, and orientation of the dispersed phase. Trying to get a better control of the final morphology, the processing of these

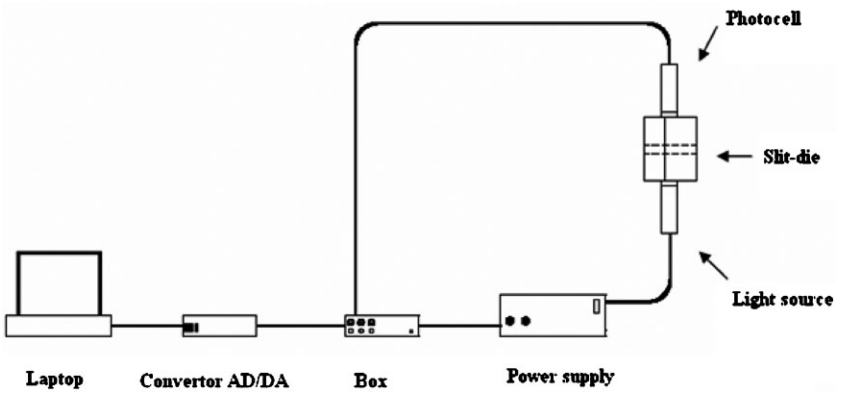

Figure 1.
Detector system.

materials has been studied in twin screw extruder, which provides great mixture capacity and short residence time when compared with single screw extruders.[14,15] These features enables twin screw extruders to be used in non-conventional processing, like reactive extrusion, polymer compounding, and controlled degradation.

PP/PA6 mixtures forms immiscible blends having phase separation, which scatters the light producing cloudy (turbid) systems. Upon compatibilization via reactive processing with e.g. PP-g-MA and PP-g-AA grafted polymers there is the reaction between the anhydride or the acid grafted PP ends with the amine PA6 end forming a PP/PA6 diblock copolymer.[16] This diblock copolymer is not miscible in nether of the phases and so migrates to the blends components interface. This positioning becomes engineeringly strategic because it reduces the interfacial tension between the phases and so allows an increase in the interfacial surface area and suppresses the coalescence of the domains, which ends up as a reduction in the particle size of the segregated minor component. Reduction in the particle size affects the optical properties increasing the turbidity of the system.

In this study, the development of a PP/PA6 blend's morphology was examinated in-line during extrusion, compatibilized with polypropylene grafted with acrylic acid (PP-g-AA). The polymers used were RP-347 polypropylene (Braskem, Brazil), Technyl poliamide 6 (Rhodia, Brazil), and Polybond 1001 PP-g-AA (Chemtura, USA). The concentration of polyamide's amine group at the chain end was 37.2 μeq/ g; this concentration was 503 μeq/ g for PP-g-AA.

The blends were prepared in a ZSK-30 modular intermeshing corotating twin-screw extruder (Werner & Pfleiderer, Germany), the melt mixing operating in the transient state. The screw configuration has two kneading blocks zones and processing conditions were kept constant: speed 75 rpm, feeding rate 2 kg/h. Once the extrusion reached a steady state, it was added a pulse made with the second phase master and completing either with the PP matrix.

The first component was the PA6, used in three different weight levels: 0.4, 0.6, and 0.8 g. The second component was the grafted compatibilizer, PP-g-AA. The ratio between the normal concentration of the functional group and that of the amine group varied widely being from zero up to 256 for the acrylic acid. A complementary amount of the PP, the same as that which forms the matrix, was added in order to keep the total weight of the pulse at a constant value of 20 g.

A constant weight minimizes differences in the residence time distribution curves due to changes in the barrel pressure that would affect adversely the level of resolution of the measurements needed for this work. The second phase is added in the flowing melt PP as a pulse and can be followed as a typical pattern of the residence time distribution (RTD) curve when exiting the extruder, through the optical detector.[10,11] A portion of the molten polymer was collected in each run, picked at the maximum pulse concentration and immediately quenched in icy water. It was later off-line analyzed by infrared spectroscopy and scanning electron microscopy to access morphology.

During the flow, the PA6 particulate second phase scatters light producing a turbid melt which is seen as the RTD curves. Figure 2 shows the normalized voltage taken from the peak of the RTD curve plotted as a function of the ratio

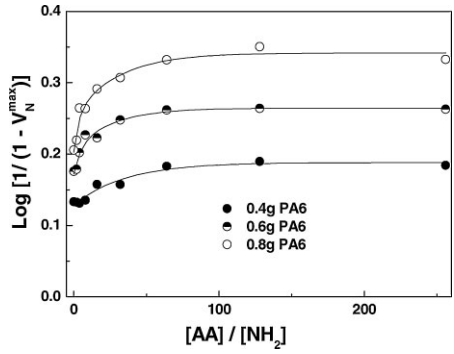

Figure 2.
Normalized detector's signal as a function of the ratio between reactive groups.

between acrylic acid and amine groups concentration. The normalized data increases with both PA6 and PP-g-AA concentrations. The greater the concentration of the dispersed PA6 particles the greater the detectoŕs response. As a second effect the compatibilizer improves the interfacial interactions between dispersed phase (PA6) and matrix (PP), decreasing the average particle size. The lower the scattering particle size the higher the scattering intensity due to the increase in the superficial area following Eq. 1.

Figure 3 shows the relation between in-line detector's normalized signal and amidic group concentration measured by FTIR (1640 cm^{-1}). Its absorbance was normalized by the peak at 1170 cm^{-1}. Data from the in-line detector show a good linear correlation with FTIR quantitative analysis. Above this concentration the amount of PA6 dispersed particles is great enough to generate multiple scattering of the light reducing the transmitted light intensity to values below then expected.

Figure 4 shows the micrographs of the PP/ PA6 blends with and without compatibilizer agent. The changes in average particle size as function of compatibilizer concentration, for pulse with 0.8 g of PA6, are shown in Figure 5. The error bars are clearly broad, but the analysis can be focused in the mean value because it represents the global effect that is captured by the in-line optical detector. The particle size decreases with an increase in the concentration of grafted copolymer.

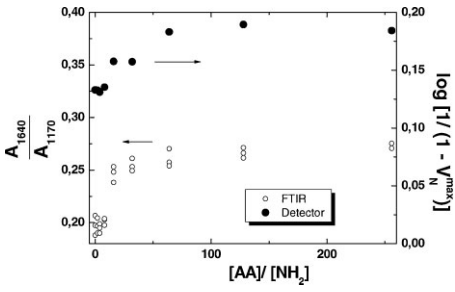

Figure 3.
Relation between detector's signal and FTIR analysis.

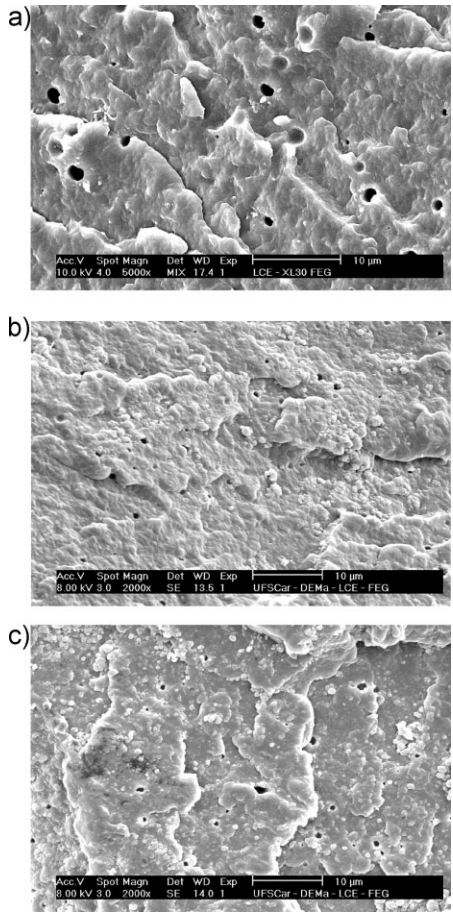

Figure 4.
PP/PA6 blend morphology compatibilized with PP-g-AA, obtained in the transient state, having pulses of PA6 with 0.8g. [AA]/ [NH_2] = : a)0; b) 8; c) 16. The scale bar in all figures is 10 μm.

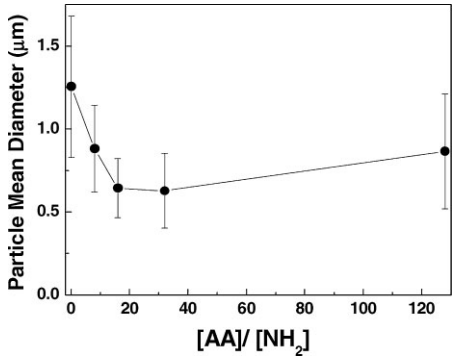

Figure 5.
Mean particle diameter in PP/PA6 blends for PP-g-AA compatibilizer.

In-line Assessment of the Melting Behaviour during Polymer Extrusion

When a tracer is dispersed in a transporting matrix its temperature is determined by the matrix thermal history on its turn affected by its properties as well as by the processing conditions adopted. Melting is an important elementary step in most polymer processing applications. Poor melting will have profound consequences on the entire process, such as discharge surging, nonuniform product, high machine wear, and coarse blend morphology. A uniform and rapid melting stage is essential in most polymer processing applications, especially in reactive polymer modification where the unmelted ''escapees'' will stay unchanged and not undergo the intended chemical reactions, leading to a product with nonuniform structure and properties.

Polymer feedstock is fed into extruders mainly in the form of solid particulates, such as pellets, powders, beads, flakes, and granules. These particulates are conveyed in a loosely packed form in the normally partially filled solids conveying section. When certain barrier elements, such as reverse screw element(s) and/or reverse/neutral kneading block(s), are installed downstream, the solid particulates get compacted and consolidated. As the pressure develops in the heating/melting section, the degree of densification of polymer particulates increases and the void ratio of the particulate assembly decreases.

A certain amount of energy has to be provided in the heating/melting section of an extruder to heat up these particulates to above their transition temperature(s). The amount of energy required for melting can be approximated from the typical specific enthalpy curve for each polymer.[17]

This energy is supplied either by heat transfer through the heated barrel walls or heat built up by dissipation. Mechanisms for heat built up in extrusion processing were very clearly depicted in the works of Gogos and coworkers.[18–21] In particular, apart from conductive heating from the extruder barrel, they identify several further sources of heat built up depending on the state of the material in the extruder, solid or melt or a mixture of the two.

When the material is still completely solid the major contributions to heat built up are provided by plastic energy dissipation (PED) and frictional energy dissipation (FED), the former related to the mechanical energy stored after plastic deformation of the solid material, the latter to the friction between solid particles sliding past each other. While viscous energy dissipation (VED) is the major contribution if the material is completely molten. In all cases the power is supplied by the mechanical energy through the extruder drive.

Experimental evidences show that PED of individual pellets in the partially filled kneading section can raise the initial temperature of polymer pellets significantly[18] This deformation energy alone can provide enough energy to heat up amorphous polystyrene (PS) pellets to above their glass transition temperature and, therefore, PS pellets may get melted in the partially filled kneading section. Although semicrystalline polypropylene (iPP) pellets cannot get melted in the partially filled kneading section, the significant temperature rise of feedstock in this region caused by the PED of individual iPP pellets contributes greatly to the subsequent melting process.

Certainly being the external temperature gradient applied to the barrel constant and being the major contributions to heat built up supplied well before the material gets melted, one can assume that the time for melting of the tracer corresponds to the time necessary for the matrix to get melted. In the case of the geometrical arrangements of the elements of the screw adopted in this work this corresponds to approximately one third of the overall residence time in the extruder.

Melting of the two polyamides tracers was studied by changing the barrel temperature and keeping all other operating conditions constant. The quantity of tracer

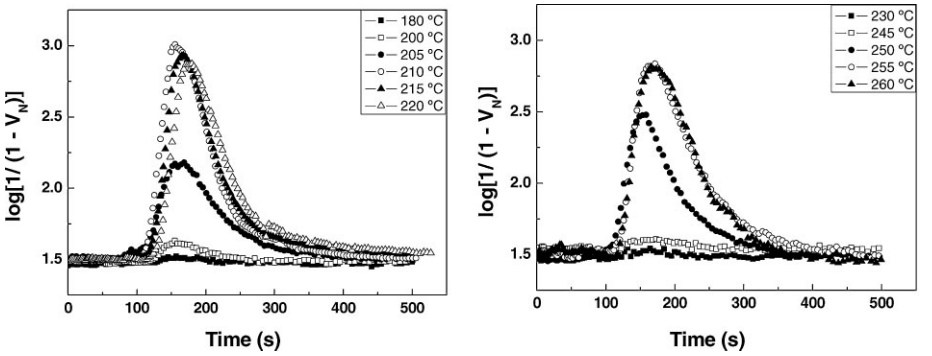

Figure 6.
Light intensity residence time in the extruder of the two tracers: PA6 and PA66.

adopted was of 0.6g for PA6 and 0.4g for PA66 such as to lie in the linear response zone as given by the calibration of the normalized light intensity at the detector tracer mass.

Upon changing the barrel temperature one observes a fast growth of the normalized intensity due to melting of the tracer scattering light, eventually saturating once all tracer is molten as Figure 6 shows. One can take the maximum slope of the normalized intensity increase as corresponding to the onset of tracer melting thus obtaining a melting temperature of 205 °C for PA6 and of 250 °C for PA66 (Figure 7).

It is clear that such melting temperatures are definitely lower, ca 15 °C, than those one could measure by a DSC heating run, according to Figure 8. It seams quite obvious to infer that such lower melting temperatures are only apparent since the heat built up due to the cited mechanisms should be responsible for the larger melting temperatures experienced by the tracers with respect to those imposed on the extruder barrel as external conditions.

For semicrystalline polymers, the case studied by Gogos et al was indeed focused on iPP, the heat built up due to PED and FED is definitely lower than for amorphous PS,[18] although it might accelerate the phase transition and the attainment of the external thermal conditions applied to the barrel, it should however be ruled out as a major player on determining the melting of the tracer in the kneading section partially filled with solid.

Therefore if melting due to heat built up is to be taken into consideration the only plausible mechanism is VED. It can arise in

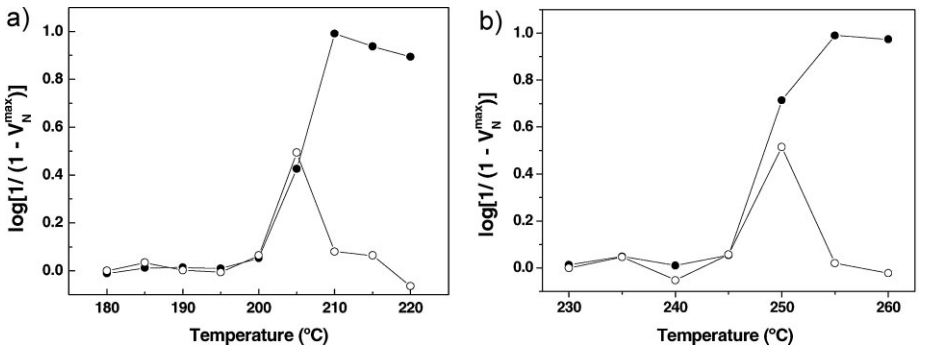

Figure 7.
Cumulative (●) and derivative (○) fraction of polymer particles melted during the extrusion as a function of the extruder set temperature: a) PA6; b) PA6,6.

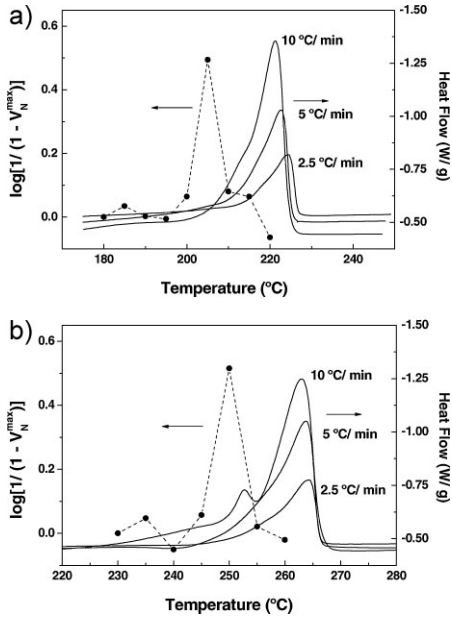

Figure 8.
Comparison between melt temperature obtained from detector (dashed lines) and DSC (solid lines), for: a) PA6; b) PA6,6.

sites where concentration of large shear stresses arises due to the presence of certain barrier elements, such as reverse screw element(s) and/or reverse/neutral kneading block(s), are installed downstream. Depending on viscosity and on the square of the deformation rate, it is significantly affected by operating conditions. Upon decreasing barrel temperature viscosity increases as well as the VED contribution to the temperature increase eventually partially balancing the lower applied external temperature, i.e. the gap between the latter and the hot spot locally generated by VED increases. It is thus questionable that the continuous increase of tracer melting observed in Figure 7 corresponds to the onset of this mechanism.

An additional plausible mechanism justifying the difference of 15 °C between the melting temperature of the PA tracers observed in the extruder by the in-line detector and by DSC may be related with the stability of crystalline lamellae and it is of general relevance to crystalline materials. It depends on the equilibrium melting temperature of finite size crystals and it is rigorously described by the Gibbs Thomson equation.[22] Lower dimension crystals will have larger surface energy contributions balancing the free melting energy such as they will melt at lower temperatures the smaller their size. The melting temperature usually determined by DSC is a fictitious value not representative of the thermal history the material has experienced during solidification. It might at most be used to identify the material. In a DSC heating run the broad melting usually observed is due to the superposition of several different mechanisms which can be summarized in a continuous melting of lower dimensional crystals of increasing size as the temperature increases, their recrystallization in larger sizes as soon as the interlamellar phase gets unconstrained due to increased mobility, finally eventually obtaining the same apparent melting temperature whatever the solidification thermal history for crystallizing the material under test was.

There are several possibilities to evaluate the importance of each of the mechanisms cited and understand if any is controlling the difference of melting temperatures observed with the two methods, further work is in progress to identify their role.

Exfoliation of the MMT Clay During the Preparation of PP/MMT Nanocomposites via Polymer melt Compounding

Nanocomposites have attracted great interest in the scientific and technological area, since they exhibit synergistic properties. One of the systems that are largely studied is the polymer-clay nanocomposite. In this class of nanocomposites the clay mineral aggregates or tactoids are reduced to single nanometer scale lamellas, depending on the compatibility of the system. The best properties are reached when the clay mineral are well dispersed in the polymeric matrix, forming an exfoliated structure.[23,24] The exfoliation is commonly

examined by X-ray diffraction and transmission electronic microscopy (MET) techniques, but others less frequent like colorimetry[25,26] and dielectric[27,28] techniques have been used to infer the exfoliation and the formation of a nanocomposite.

The in-line optical method was used to measure exfoliation level in a PP/ montmorilonite (MMT) nanocomposite. The light extinction level measured by the intensity of the detector's signal is dependent upon the clay type (organofilization treatment), concentration and particle size (only in the range of 0.2 to 10 microns to get extinction). The clay tactoids can be detected because their size is in the light extinction range. On tactoid exfoliation its size is reduced below the minimum particle size to produce light extinction (turbidity) and so the signal intensity reduces as the nanosize composite is formed.

The materials used were: PP homopolymer (H 301) from Braskem - Brazil, PP-g-MA (Polybond 3200) from Chemtura – USA and the commercial modified MMT clays (Cloisite® (Na^+, 20A, 15A, 30B)) from Southern Clay Products Gonzales/ TX. To produce a new clay type Cloisite® 20A was sintered in an oven for 2 hours at 600 °C, called ''Sintered''.

A concentrated mixture or master were prepared in a internal mixer Torque Rheometer (Haake Rheomix 600) during 4 min at 180 °C, 100 rpm with 33 wt. % MMT for master PP/MMT and 25 wt.% MMT for PP-g-MA/MMT master. Prior using the modified clays was dried in a vacuum oven for 24h at 80 °C.

The PP/MMT nanocomposite was prepared in a ZSK-30 modular intermeshing corotating twin-screw extruder (Werner & Pfleiderer, Germany), the melt mixing operating in the transient state. Two screw configurations were used: one with a higher shear intensity (ROS) e the other with a low shear intensity (2KB90). Processing conditions were: speed 100 rpm, feeding rate 2 kg/h, and temperature was 190 °C in all the heating zones. Once the extrusion reached a steady state, it was added a 4g total pulse weight. All the pulses were made to keep the same proportion of MMT and compatibilizer (1:3). The pulse for the PP/ MMT master were made of 2 g of master plus compatibilizer or PP matrix or for the PP-g-MA/MMT master made of 2,667 g of master plus 1,333 g of PP.

The morphology of the nanocomposites was examined using wide-angle X-ray (WAXS) scattering. WAXS scans were performed in the reflection mode at a scan rate of 1°/min using a Rigaku Multiflex diffractometer.

The MMT concentration calibration was conducted in the extruder operating in the stead state. A PP/ MMT master pellets were tumbled-mixed with PP and fed into the extruder. The MMT used is Cloisite® Na^+, chosen because it is assumed that it is not able to exfoliate due to the lack of the organofilic treatment. The detector's signal quantifies the clay fraction that has not been exfoliated during the melt compounding. Figure 9 shows the calibration curve of the normalized light extinction as a function of the clay concentration added in the composite. It is a linear function obtained in the range of the data obtained in the transient state and showed in Figure 10.

Figure 10 shows a comparison of the normalized maximum light extinction obtained for various PP/MMT transient nanocomposites with the same initial MMT concentration.

The different clay organofilization treatments generate different concentrations of unexfoliated tactoids. As expected the

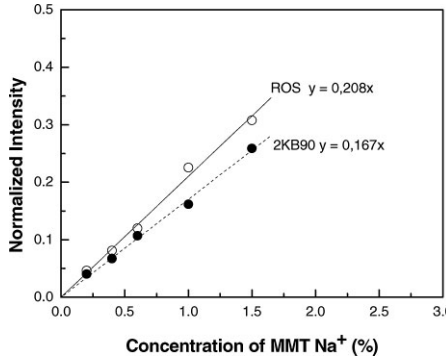

Figure 9.
Calibration curve for screw profile ROS and 2KB90.

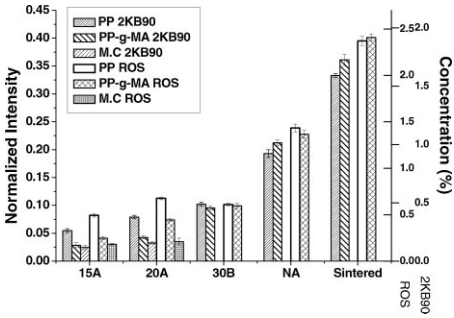

Figure 10.
In-line measurements using different clays, processed in the screw profiles 2KB90 e ROS using the compatibilizer or not with the PP/MMT master or using the master PP-g-MA (M.C) with PP matrix.

''sintered'' clay presents the maximum light extinction as the organo-modification was removed. The extinction level is very high, outside the linear calibrated range, producing a PP/ MMT black (micro)composite. The same is seen for the Cloisite® Na^+ indicating a minimum exfoliation level, if any. In both cases the presence of the PP-g-MA compatibilizer is useless.

Preparing PP/ MMT nanocomposites in the transient state with organo-modified clays the light extinction is greatly reduced indicating that the tactoids were exfoliated to a great efficiency. In the case of Cloisite® 30B, which has been recommended to be used in polar polymer matrixes, the level of turbidity (light extinction) is quite high indicating lower exfoliation. The presence of the PP-g-MA compatibilizer has contributed to some clay tactoids desagglomeration but still at a non-effective level.

On the other hand the use of Cloisite® 20A and Cloisite® 15A, mainly used in nonpolar polymer matrixes, has shown a low normalized maximum light extinction indicating a great level of exfoliation which is improved even still with the presence of the PP-g-MA compatibilizer. A partial desagglomeration of the initial MMT tactoids have been achieved which can be successfully quantified using the proposed in-line optical monitoring method.

For Cloisite® 20A and Cloisite® 15A the influence of the master preparation process was also examined. The use of the master PP-g-MA/ MMT shows a lower normalized light extinction than the master PP/ MMT, indicating that the exfoliation process had already begun in the internal mixer and during the melt flow the clay is just diluted into the PP matrix. The Cloisite® 20A is more affected the way the master was prepared.

The morphology of the nanocomposites was investigated by WAXS. The difratograns for Cloisite® 15A and Cloisite® 20A are shown in Figure 11 because for this clays the in-line monitoring have achieved a higher exfoliation level.

The results show that the morphology achieved is intercalated/ exfoliated, because the pristine clay diffraction peak is shifted to lower angles and its intensity decreases. When the master is prepared with the compatibilizer in the internal

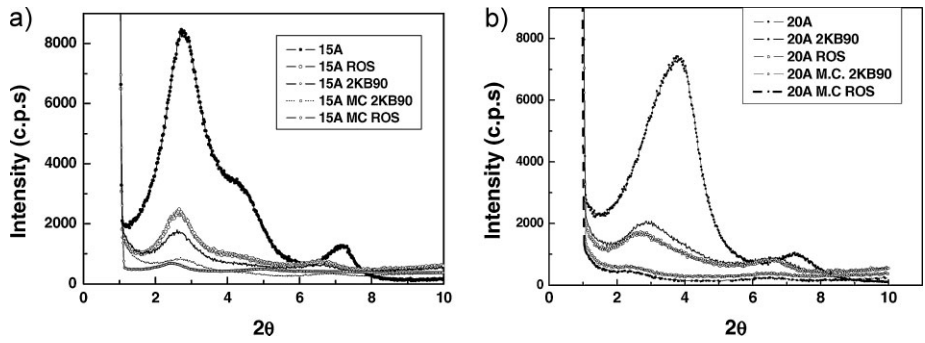

Figure 11.
Difratogram of a) Cloisite® 15A and b) Cloisite® 20A for the different processing methods

mixer, the intercalated/ exfoliated morphology of the nanocomposite is obtained more efficiently.

The turbidity measurements are in agreement with the WAXS results, providing a new quantitative technique to monitor in-line the formation of a nanocomposite during melt mixing.

Conclusions

In-line detection fitted at the extruder die exit is a reliable means of following in real time changes in the morphology of the melt flowing stream. The use of an optical detector allows the measurement of the turbidity produced by the light scattering on the segregated second phase which can be measured and related to its concentration, type and particle size. In this paper we have shown the use of an optical in-line detection system to follow the formation of polymer blends (PP/PA6) and nanocomposites (PP/MMT), studying the effect of compatibilizers, tactoids desegregation and the level of viscous heating during polymer melt blending.

Acknowledgements: The authors would like to thank CNPq, CAPES and FAPESP (projeto temático 2006/61008-5) for the financial support, Braskem for the donation of the PP, Rhodia for the donation of PA6 and PA6,6, and Crompton for the donation of the PP-g-AA and PP-g-MA.

[1] Z. J. Chen, R.-J. Wu, M. T. Shaw, R. A. Weiss, *Polym. Eng. Sci.* **1995**, *35*, 92.
[2] M. G. Hansen, A. Khetrry, *Polym. Eng. Sci.* **1994**, *34*, 1758.
[3] K. Sano, M. Shimoyama, M. Ohgane, H. Higashiyama, M. Watari, M. Tomo, T. Ninomiya, Y. Ozaki, *Appl. Spectrosc.* **1999**, *53*, 551.
[4] T. Rohe, W. Becker, S. Kölle, N. Eisenreich, P. Eyerer, *Talanta* **1999**, *50*, 283.
[5] G. Schlatter, C. Serra, R. Bouquey, R. Muller, J. Terrisse, *Polym. Eng. Sci.* **2002**, *42*, 1965.
[6] P. D. Coates, S. E. Barnes, M. G. Sibley, E. C. Brown, H. G. M. Edwards, I. J. Scowen, *Polymer* **2003**, *44*, 5937.
[7] T. J. A. Mélo, S. V. Canevarolo, *Polym. Eng. Sci.* **2002**, *42*, 170.
[8] T. J. A. Mélo, S. V. Canevarolo, *Polímeros* **2002**, *12*, 255.
[9] T. J. A. Mélo, S. V. Canevarolo, *Polym. Eng. Sci.* **2005**, *45*, 11.
[10] L. A. Pinheiro, C. S. Bitencourt, L. A. Pessan, S. V. Canevarolo, *Macromol. Symp.* **2006**, *245–246*, 347.
[11] L. A. Pinheiro, G.-H. Hu, L. A. Pessan, S. V. Canevarolo, *Polym. Eng. Sci.* **2008**, *48*, 806.
[12] G. H. Meeten, "*Optical Properties of Polymers*", Elsevier, London **1986**.
[13] L. H. Sperling, "*Poymeric multicomponent materials: an introduction*", John Wiley & Sons, New York **1997**.
[14] Dreiblat, K. Eise, Intermeshing corotating twin-screw extruders, in: C. Rauwendaal, Ed., "*Mixing in polymer processing*", Marcel Dekker, New York **1991**, p. 241–265.
[15] Rauwendaal, "*Polymer extrusion*", 2nd ed., Hanser Publishers, München **1990**.
[16] J. Roeder, R. V. B. Oliveira, M. C. Gonçalves, V. Soldi, A. T. N. Pires, *Polym. Test.* **2002**, *21*, 815.
[17] B. Wunderlich et al. Advanced Thermal Analysis System (ATHAS) http://www.prz.rzeszow.pl/athas/
[18] C. G. Gogos, Z. Tadmor, M. H. Kim, *Adv. Polym. Tech.* **1998**, *17*, 285.
[19] B. Qian, C. G. Gogos, *Adv. Polym. Tech.* **2000**, *19*, 287.
[20] C. G. Gogos, B. Qian, *Adv. Polym. Tech.* **2002**, *21*, 287.
[21] C. G. Gogos, B. Qian, *Adv. Polym. Tech.* **2003**, *22*, 85.
[22] B. Wunderlich, "*Thermal Analysis of Polymeric Materials*", Springer, Berlin **2005**.
[23] M. Alexandre, P. Dubois, *Mater. Sci. Eng.* **2000**, *28*, 1.
[24] S. S. Ray, M. Okamoto, *Prog. Pol. Sci.* **2003**, *28*, 1539.
[25] T. D. Fornes, P. J. Yoon, D. R. Paul, *Polymer* **2003**, *44*, 7545.
[26] P. J. Yoon, D. L. Hunter, D. R. Paul, *Polymer* **2003**, *44*, 5341.
[27] R. D. Davis, A. J. Bur, M. McBrearty, Y. H. Lee, J. W. Gilman, P. R. Start, *Polymer* **2004**, *45*, 6487.
[28] A. J. Bur, Y. H. Lee, S. C. Roth, P. R. Start, *Polymer* **2005**, *46*, 10908.

